



HHS Public Access

Author manuscript

Clin Nutr. Author manuscript; available in PMC 2022 April 01.

Published in final edited form as:

Clin Nutr. 2021 April ; 40(4): 2053–2060. doi:10.1016/j.clnu.2020.09.028.

Metabolomic Basis for Response to High Dose Vitamin D in Critical Illness

Karin Amrein, MD, MSc,

Division of Endocrinology and Diabetology, Medical University of Graz, Graz, Austria

Jessica A. Lasky-Su, ScD,

Channing Division of Network Medicine, Brigham and Women's Hospital, USA

Harald Dobnig, MD,

Thyroid Endocrinology Osteoporosis Institute Dobnig, Graz, Austria

Kenneth B. Christopher, MD, SM

Division of Renal Medicine, Channing Division of Network Medicine, Brigham and Women's Hospital, USA

Abstract

Background & Aims: It is unclear if intervention can mitigate the dramatic alterations of metabolic homeostasis present in critical illness. Our objective was to determine the associations between increased 25-hydroxyvitamin D levels following high dose vitamin D₃ and more favorable metabolomic profiles in critical illness.

Methods: We performed a post-hoc metabolomics study of the VITdAL-ICU randomized double-blind, placebo-controlled trial. Trial patients from Medical and Surgical Intensive Care Units at a tertiary university hospital with 25-hydroxyvitamin D level ≥ 20 ng/mL received either high dose oral vitamin D₃ (540,000 IU) or placebo. We performed an analysis of 578 metabolites from 1215 plasma samples from 428 subjects at randomization (day 0), day 3 and 7. Using mixed-effects modeling, we studied changes in metabolite profiles in subjects receiving intervention or placebo relative to absolute increases in 25-hydroxyvitamin D levels from day 0 to day 3.

Results: 55.2% of subjects randomized to high dose vitamin D₃ demonstrated an absolute increase in 25-hydroxyvitamin D ≥ 15 ng/ml from day 0 to day 3. With an absolute increase in 25-hydroxyvitamin D ≥ 15 ng/ml, multiple members of the sphingomyelin, plasmalogen, lysoplasmalogen and lysophospholipid metabolite classes had significantly positive Bonferonni

Corresponding Author: Kenneth B. Christopher, MD, SM, Division of Renal Medicine, Channing Division of Network Medicine, Brigham and Women's Hospital, 75 Francis Street, Boston, MA 02115 USA, kbchristopher@bwh.harvard.edu c. 617 272 0535.

Statement of Authorship

Drs. Christopher and Amrein had full access to all the data in the study and take responsibility for the integrity of the data and the accuracy of the data analysis. Study concept and design: Amrein, Lasky-Su, Christopher. Acquisition, analysis, or interpretation of data: All authors. Drafting of manuscript: All authors. Statistical analysis: Amrein, Lasky-Su, Christopher. Obtained funding: Amrein, Dobnig, Christopher. Administrative technical or material support. All authors. Study Supervision: Amrein, Dobnig, Christopher.

Conflict of Interest Statement

Dr. Amrein reports receiving lecture fees from Fresenius Kabi. Dr. Dobnig reports receiving lecture fees from Fresenius Kabi. No other financial or other relationships exist that might lead to a conflict of interest.

corrected associations over time. Further, multiple representatives of the acylcarnitine and phosphatidylethanolamine metabolite classes had significantly negative Bonferonni corrected associations over time with an absolute increase in 25-hydroxyvitamin D ≥ 15 ng/ml. Changes in these highlighted metabolite classes were associated with decreased 28-day mortality.

Conclusions: Increases in 25-hydroxyvitamin D following vitamin D₃ intervention are associated with favorable changes in metabolites involved in endothelial protection, enhanced innate immunity and improved mitochondrial function.

Keywords

Metabolite; Metabolomics; Vitamin D; Critical Illness; sphingomyelin; plasmalogen; lysoplasmalogen; lysophospholipid; acylcarnitine; phosphatidylethanolamine

Introduction

Critical illness is a dramatic disruptor of metabolic homeostasis where circulating metabolic profiles are the products of the cellular response to oxidative stress and inflammation [1]. Metabolic profiles predictive of critical illness severity and outcomes are identifiable early in critical illness [2]. The effect of treatment on the metabolic disruption of critical illness is not known.

The VITdAL-ICU trial was a double-blind, placebo-controlled, single-center trial of 492 critically ill adults with 25-hydroxyvitamin D [25(OH)D] levels ≤ 20 ng/ml to high dose oral vitamin D₃ conducted from 2010 to 2012 [3]. The VITdAL-ICU trial was negative for the primary outcome of length of stay and the secondary outcomes hospital mortality and 6-month mortality. Though only half of VITdAL-ICU subjects who received high dose oral vitamin D₃ demonstrated the expected increase in 25(OH)D levels ≥ 30 ng/ml, a subgroup analysis showed significant improvement in mortality in those with very low vitamin D levels [3].

As metabolomic profiles can distinguish critically ill patients with and without low 25(OH)D levels [4] and vitamin D receptor may regulate expression of up to 5% of the total human genome [5], we determined whether high dose oral vitamin D alters the metabolomic landscape of critical illness over time. We conducted a post-hoc metabolomics study on plasma samples from the VITdAL-ICU trial (NCT01130181) [3]. We hypothesize that significant differences in metabolomic profiles exist in patients who demonstrate an increase in plasma 25(OH)D levels following randomization to high dose vitamin D₃, and these changes are associated with clinical benefit.

Methods

Detailed methods are presented in Supplemental Methods. The VITdAL-ICU trial randomized 475 critically ill adult patients with 25(OH)D < 20 ng/mL to vitamin D₃ or placebo given orally or via nasogastric tube once at a dose of 540,000 IU followed by 90,000 IU monthly [3]. The trial was conducted at the University Hospital Graz in Southeast Austria in 5 Medical and Surgical Intensive Care Units. Patients were randomized 1:1 with

randomization block size of 8 stratified via Intensive Care Unit type and sex. The primary study outcome was length of hospital stay. Secondary outcomes included 28-day mortality, hospital mortality, 6-month mortality, length of Intensive Care Unit (ICU) stay and 25(OH)D levels at day 0, 3 and 7. Whole blood was collected at randomization (day 0), day 3 and day 7. Plasma was fractionated, aliquoted and stored at -70°C . At VITdAL-ICU trial enrollment, written informed consent was obtained, if possible, directly from the patient or from a legal surrogate. Consent included permission for plasma specimens to be saved for future research studies. The post-hoc study research protocol was approved by the Partners Human Research Committee at the Brigham and Women's Hospital.

Our exposure of interest was the absolute increase in 25(OH)D levels from randomization (day 0) to day 3. 453 trial subjects had frozen plasma available for analysis. We excluded 25 trial subjects who did not have 25(OH)D measured at day 3 following randomization. A total of 1215 plasma samples from 428 patients at day 0, 413 patients at day 3 and 374 patients at day 7 were analyzed using four ultra high-performance liquid chromatography/tandem accurate mass spectrometry methods by Metabolon, Inc. in 2017. Metabolomic profiling identified 769 metabolites. We reduced baseline noise by removing metabolites with the lowest interquartile range of variability, leaving 578 metabolites [6]. Metabolomic data underwent a cube root transformation followed by Pareto scaling to generate data that were on the same scale followed an approximate normal distribution [7]. In our tables, we follow the metabolite identification criteria level described by Sumner et al: Level 1 is a validated identification against a pure reference standard and Level 2 is a recognized identification with predictive or externally acquired structure evidence [8].

For univariate analysis of pre-randomization data (day 0), Student's t test was used to determine the significance of each metabolite between groups with False Discovery Rate (FDR) adjusted p-values using MetaboAnalyst 4.0 [9]. Pre-randomization data were also analyzed using orthogonal partial least square-discriminant analysis (OPLS-DA), a supervised method to assess the significance of classification discrimination (SIMCA 15.0 Umetrics, Umea, Sweden). The quality of the multivariate OPLS-DA model developed was described by R2 and Q2 corresponding to goodness of fit and predictive performance, respectively. Permutation testing was performed to validate the OPLS-DA model [10, 11]. Sevenfold cross-validation analysis of variance (CV-ANOVA) was utilized to determine OPLS-DA model significance [11].

For repeated measures data (day 0, 3 and 7), the association between relative quantitation of individual metabolites (outcome) over time and absolute increase in 25(OH)D levels from baseline day 0 to day 3 were determined utilizing linear mixed-effects models correcting for age, sex, baseline 25(OH)D, Simplified Acute Physiology Score (SAPS) II, admission diagnosis category and plasma day (as the random-intercept). For data visualization purposes, a bipartite graph [12] was generated of metabolites that were significantly changed (increased or decreased) with the absolute increase in 25(OH)D levels from baseline day 0 to day 3. Mixed-effects logistic regression was used to estimate the odds of 28-day mortality relative to the abundance of individual metabolites adjusted for absolute increase in 25(OH)D, age, sex, baseline 25(OH)D, SAPS II, admission diagnosis category and plasma day (as the random-intercept). Further, for repeated measures plasma

data (day 0, 3 and 7), the association between relative quantitation of individual metabolites (outcome) over time and high dose vitamin D₃ randomization (binary) was determined utilizing linear mixed-effects models correcting for age, sex, baseline 25(OH)D, SAPS II, admission diagnosis category and plasma day (as the random-intercept).

Additionally, we assessed the association between individual metabolites and absolute increase of plasma 25(OH)D between day 0 and day 3 to levels of 2.5, 5.0, 7.5, 10.0, 12.5, 15.0, 17.5 or 20.0 ng/ml. For each absolute increase cut point (i.e. 2.5 ng/ml), we utilized linear mixed-effects models correcting for age, sex, baseline 25(OH)D, SAPS II, admission diagnosis category and plasma day (as the random-intercept). A Bonferroni multiple testing correction threshold of $p < 8.65 \times 10^{-5}$ (p of 0.05/578 metabolites per plasma sample) was used to identify all significant mixed-effects associations [13]. All mixed-effects models were analyzed using STATA 14.1MP (College Station, TX). We employed rain plots [14] to visualize effect size, significance, clustering and trends across days 0, 3 and 7. Rain plots were produced based on hierarchical clustering in R-3.6.2.

As organ function is important in oral vitamin D₃ pharmacokinetics, we evaluated a potential mediating effect of creatinine or bilirubin on the association between the absolute increase in 25(OH)D levels from randomization (day 0) to day 3 and individual metabolite abundance adjusted for age, sex, baseline 25(OH)D, SAPS II and admission diagnosis. Analyses were performed on each of the 578 metabolites at day 3 using the R package mediation [15] to obtain bootstrap P values (N = 2000 samples) for the mediation effect of creatinine or bilirubin. Significant mediation was present if the p value was < 0.01 and 10% or more of the association was mediated through creatinine or bilirubin levels [16, 17].

Results

In the analytic cohort, the mean (SD) and median [IQR] increase in 25(OH)D level between day 0 and day 3 were 10.4 (16.4) ng/ml and 3.15 [0,16.5] ng/ml respectively. Baseline characteristics of the analytic cohort were balanced between subjects in quartiles of absolute increase in 25(OH)D level between day 0 and day 3 for age, sex, C-reactive protein and SAPS II. Differences existed in the quartiles of absolute increase in 25(OH)D level between day 0 and day 3 with respect to baseline 25(OH)D levels, Day 0 total bilirubin and creatinine, intervention status, ICU type and admission diagnosis category (Table 1 and Supplemental Table 1). The overall 28-day mortality of the 428 subject analytic cohort was 22.2%.

In day 0 plasma samples (N=428), no significant differences exist in 578 individual metabolites [all False Discovery Rate (FDR) adjusted p-values > 0.99] or in OPLS-DA metabolomic profiles (CV-ANOVA p value=1.00) in subjects randomized to high dose vitamin D₃ or placebo (Supplemental Table 2). In day 0 plasma samples (N=428), significant differences exist in 53 individual metabolites (all FDR adjusted p-values < 0.05) but not in OPLS-DA metabolomic profiles (CV-ANOVA p value=1.00) in subjects with or without mortality at 28 days (Supplemental Tables 2 & 3).

Next we evaluated metabolic changes with respect to absolute increases in plasma 25(OH)D levels. Mixed-effects modeling of 1215 plasma samples from day 0, 3 and 7 from 428 subjects, highlighted 133 significant metabolites. Forty-one metabolites had significantly positive associations with an absolute increase in 25(OH)D level between day 0 and day 3. These 41 metabolites were dominated by increases in multiple representatives of each of the following lipid classes: sphingomyelins, plasmalogens, lysoplasmalogens and lysophospholipids (Table 2, Supplemental Table 4 & Figure 1). Abundance of 22 of these 41 metabolites were significantly associated with decreases in 28-day mortality (Supplemental Table 5). Ninety-two metabolites had significantly negative associations with an absolute increase in 25(OH)D level, primarily by decreases in multiple representatives of the acylcarnitine, phosphatidylethanolamine and amino acid class metabolites (Table 3, Supplemental Table 6 & Figure 1). Decreases of 81 of these 92 metabolites were significantly associated with decreases in 28-day mortality (Supplemental Table 7). Addition of C-Reactive Protein at day 0 or total bilirubin or creatinine to the mixed-effects linear and logistic models did not alter the direction and significance of the observations (data not shown). With fidelity to the intention to treat analysis, mixed-effects modeling of the 1215 plasma samples from day 0, 3 and 7 from 428 subjects demonstrated no metabolites had significantly positive or negative associations in subjects randomized to high dose vitamin D₃ relative to placebo.

We subsequently determined if the identified metabolic changes with respect to absolute increases in plasma 25(OH)D levels differ between subjects who received high dose vitamin D₃ versus those who received placebo. We repeated the mixed-effects modeling restricted to subjects who received high dose vitamin D₃ (N=212) or to subjects that received placebo (N=216). In subjects who received high dose vitamin D₃ (N=212), mixed-effects modeling of plasma samples from day 0, 3 and 7 show all but one of the 133 metabolites highlighted in the full 428 subject cohort (Supplemental Tables 4 & 6) had significant associations with an absolute increase in 25(OH)D level between day 0 and day 3 (Supplemental Tables 8 & 9). Conversely, in subjects who receive placebo (N=216), mixed-effects modeling of plasma samples from day 0, 3 and 7 show that only two of the metabolites highlighted in the full cohort (Supplemental Tables 4 & 6) had significant associations with an absolute increase in 25(OH)D level between day 0 and day 3 (Supplemental Tables 8 & 9).

As the VITdAL-ICU trial showed significant improvement in 28-day mortality only in subjects with baseline 25(OH)D ≥ 12 ng/ml [3], we next restricted our mixed-effects analysis to those 181 subjects with 25(OH)D ≥ 12 ng/ml at day 0. Though underpowered, in mixed-effects modeling of 525 plasma samples from day 0, 3 and 7 from 181 subjects, 14 metabolites had significantly positive mixed-effects associations with an absolute increase in 25(OH)D level. These changes were dominated by increases in multiple representatives of sphingomyelin, plasmalogen, and lysoplasmalogen class metabolites (Supplemental Table 8). Twenty-one metabolites had significantly negative mixed-effects associations with an absolute increase in 25(OH)D level, primarily by decreases in multiple representatives of the acylcarnitine and amino acid class metabolites (Supplemental Table 8). Restriction of our mixed-effects analysis to only those 212 subjects assigned to high dose vitamin D₃ showed a similar association pattern (data not shown).

We next explored the relationship between the magnitude of the absolute increase in 25(OH)D levels between day 0 and day 3 and changes in metabolites over time. The pattern of change in metabolite profiles associated with an absolute increase in 25(OH)D ranging from 2.5 to 20.0 ng/ml was demonstrated in mixed-effects modeling of the 1215 plasma samples from the analytic cohort obtained on day 0, 3 and 7 from 428 subjects. The rain plot (Figures 2 & 3) shows the separation of metabolites that are increased (red) or decreased (blue) and shows the magnitude of significance by the size of the circles with larger circles denoting higher significance. Subjects who have absolute increases in 25(OH)D \geq 10 ng/ml between day 0 and 3, show significant changes of a few sphingomyelins, plasmalogens, lysoplasmalogens, lysophospholipids, and acylcarnitines (Figures 2 and 3). With the absolute increase in 25(OH)D \geq 15 ng/ml between day 0 and 3, we observe a large number of significant changes in metabolite class members including sphingomyelin, plasmalogen, lysoplasmalogen, lysophospholipid, and acylcarnitine (Figures 2 and 3). Further, decreased 28-day mortality rates are observed with increases in 25(OH)D levels between day 0 and 3. The lowest mortality is found in subjects with an increase in 25(OH)D \geq 17 ng/ml between day 0 and 3 (Supplemental Table 9).

We finally focused on the potential mediation of the relationship between metabolite abundance and absolute increase in 25(OH)D level between day 0 and day 3 by organ function. Mediation analyses in day 3 data revealed no influence of serum creatinine on associations between the absolute increase in 25(OH)D and all 578 metabolites. With regard to bilirubin, mediation analyses in day 3 data revealed a significant influence on associations between the absolute increase in 25(OH)D levels and 100 of the 578 individual metabolites (all p values were $<$ 0.01 and the proportion mediated was over 10% using 2000 bootstrap samples). Eighty of these mediated metabolites were also identified in our mixed-effects analysis as significantly changed with absolute increases in 25(OH)D (Supplemental Figure 1). None of the sphingomyelins or short-chain acylcarnitines (C2-C7) are mediated by bilirubin.

Discussion

Interventional trials in critical illness frequently fail. The multiple potential reasons for failure include that the intervention does not work, cohort heterogeneity, insufficient power, high or low severity of illness, pleiotropic effects of the intervention, delta inflation, improper primary outcome and patient response to therapy [18–20]. These issues are evident in the major negative critical illness trials in high dose vitamin D₃ supplementation, the VITdAL-ICU and VIOLET trials [3, 21]. In the VITdAL-ICU and VIOLET trials, of those randomized to high dose vitamin D₃, 50% and 25% of subjects respectively did not have a normalization of 25(OH)D levels (\geq 30 ng/ml at day 3), biasing the trials towards the null [3, 21–23]. The VITdAL-ICU and VIOLET trials enrolled patients with 25(OH)D $>$ 12 to 20 ng/ml, a group that may not benefit from high dose vitamin D₃ [24]. The VIOLET trial was designed to study subjects at high risk for ARDS but randomized subjects with mild critical illness of which only 8% had ARDS [24]. Improvement of critically ill patient-centered outcomes following high dose vitamin D₃ supplementation has yet to be proven [3, 21].

The VITdAL-ICU trial used an enrichment strategy by only randomizing subjects with low 25(OH)D levels yet significant improvement in mortality only occurred in a subset of subjects with 25(OH)D \geq 12 ng/ml [3]. Using a novel approach of applying metabolomics to a large clinical trial biorepository, we studied the subject metabolomic response to intervention over time. We identified differences in the metabolome of subjects who responded to vitamin D₃ with an increase in 25(OH)D versus those who did not. A large proportion of metabolites that changed with an increase in 25(OH)D were also found to be associated with improved outcomes. Such examination into how the metabolites of subjects respond to intervention over time allows for an effective utilization of biospecimens to produce a more nuanced understanding of the parent clinical trial.

We find that at randomization the intervention and placebo groups are not statistically different with respect to metabolomic profiles but significant differences are present relative to 28-day mortality. We demonstrate in mixed-effects analyses that significant metabolomic changes over time are present relative to the absolute increase in plasma 25(OH)D level. Absolute increases in plasma 25(OH)D are associated with metabolomic profiles with increases in sphingomyelins, plasmalogens, lysoplasmalogens and lysophospholipids as well as decreases in acylcarnitines, phosphatidylethanolamines and amino acid metabolites (Figure 1). In vivo work shows that these metabolomic changes are consistent with endothelial protection, enhanced innate immunity and improved mitochondrial function [25–28]. These observed changes occurred in multiple metabolite members from each highlighted sub-pathway and were associated with improvement in 28-day mortality (Supplemental Tables 5 & 7). We also find that at an absolute increase in plasma 25(OH)D level of 15–17.5 ng/ml, the metabolomic changes are most robust (Figures 2 & 3). The associations between the absolute increase in 25(OH)D levels and the abundance of metabolites are significantly influenced by serum total bilirubin. Such mediation is likely reflective of 25(OH)D production being regulated by the liver cytochrome P450 2R1 [29] and the widespread expression of vitamin D receptors in liver nonparenchymal cells [30, 31].

We observe similar significant patterns of metabolomic profile changes in mixed-effects analyses of the analytical cohort as when subjects are restricted to those with baseline 25(OH)D \geq 12 ng/ml or restricted to only high dose vitamin D₃ intervention subjects with respect to absolute increase in 25(OH)D level. Further, when studied in an intention-to-treat (ITT) fashion, metabolomics differences were absent. This is not unexpected as a low proportion of subjects (55.2%) had an absolute increase in 25(OH)D level \geq 15 ng/ml three days following high dose vitamin D₃ (Supplemental Table 9). While at this 25(OH)D level \geq 15 ng/ml threshold metabolite changes are abundant (Figures 2 & 3), the high percentage of subjects with little absolute change in 25(OH)D levels biases the ITT analyses to the null [23].

The increases in sphingomyelins, plasmalogens and lysophospholipids are reflective of the stress response, antioxidants and immunomodulation respectively. Sphingomyelins are signaling mediators of the response to cellular stress and inflammation. Vitamin D₃ induces sphingomyelin turnover [32] through activation of sphingosine kinase and inhibition of ceramide-induced apoptosis [33]. Plasmalogens function as antioxidants to protect the

endothelium from oxidative stress and injury by limiting toxic oxidation products [25]. Lysophospholipids are multifactorial signaling molecules with powerful immune modulation and chemoattractant effects. Lysophospholipids released from apoptotic cells act to recruit monocytes and macrophages [34, 35] leading to clearance of apoptotic cell debris limiting immune system activation by secondary necrosis [28].

In critical illness, metabolic pathways are altered to preferentially catabolize fatty acids and amino acids. Elevated short-chain acylcarnitines (C2-C7) [36] found in plasma are due to incomplete mitochondrial fatty acid β -oxidation and suggestive of impaired mitochondrial function [37]. Vitamin D is important in the regulation of mitochondrial function [38] as well as the control of fatty acid composition in adipose tissue [39]. Further, vitamin D₃ therapy is noted to improve mitochondrial oxidative function in vitamin D-deficient adults [40]. Thus the decrease in plasma short-chain acylcarnitines associated with an absolute increase in 25(OH)D level in our study may reflect more efficient fatty acid β -oxidation thorough improved mitochondrial bioenergetics.

Our observation of decreases in plasma phosphatidylethanolamines with absolute increases in 25(OH)D levels may be reflective of endothelial protection leading to less endothelial dysfunction. Circulating phosphatidylethanolamines are found on the surface of microparticles derived from endothelium and white blood cells [41]. In experimental models, circulating phosphatidylethanolamines are increased following endothelial cell exposure to oxidative stress and also in response to sepsis [26, 27]. Decreased phosphatidylethanolamine is also noted with vitamin D administration in experimental studies [42].

Our methodology has several strengths. We utilized a novel approach to producing high quality large-scale metabolomic time-series data from a randomized trial. Our design allowed for exploration of the variable subject response to high dose vitamin D₃ as reflected in 25(OH)D levels, an unforeseen gap in trial study design [43]. We employ linear mixed-effects models which are robust analysis tools for metabolomics studies with repeated time points and multiple sources of clinical variation [44, 45]. Our approach allows for a focus on metabolites that change with response to vitamin D₃ rather than rather than just the natural course of critical illness. To limit false positive observations, we conservatively adjusted our mixed-effects significance threshold to account for 578 multiple comparisons [13, 46]. Further, prior in vitro studies demonstrate the importance of vitamin D₃ on sphingomyelins, phosphatidylethanolamines and mitochondrial oxidative function thus increasing the relevance and biological plausibility of our observations [32, 33, 38, 40, 42].

Our study does have potential limitations. The overall negative results of the VITdAL-ICU trial may be related to the heterogeneity of the subjects, their underlying disease or severity of illness which may all factor into serum 25(OH)D levels. The VITdAL-ICU trial was underpowered for mortality with differences in mortality found only in a subgroup analysis which may increase the probability of Type II and Type I errors respectively. When adherence or response to intervention is not perfect as in the VITdAL-ICU trial, intention-to-treat (ITT) analysis attenuate the causal effect estimates of an intervention [23].

Thus we also employed non-ITT analyses to study the association of the absolute increase in 25(OH)D and metabolite change [47]. Despite multivariable adjustment, our approach using nonrandomized comparisons is subject to bias as subjects with increases in 25(OH)D following vitamin D₃ may be systematically different. Our study is a post-hoc analysis of blood samples where we performed a posteriori statistical tests with compensation for multiple testing. As such, our observations should be considered hypothesis generating. Further, the single-center setting may limit generalizability of our findings. Finally, although the function and biological relevance of a metabolite may be known, the clinical significance may not be.

Conclusions

Personalized medicine holds promise for a tailored targeted approach in critical care. Our study demonstrates that VITdAL-ICU trial subjects with absolute increases in 25(OH)D levels following vitamin D₃ have dramatic coordinated changes towards more favorable metabolomic profiles. Our observations suggest that VITdAL-ICU trial subjects with absolute increases in 25(OH)D levels following vitamin D₃ have significant changes of metabolomic profiles of the same sub-pathways which are associated with decreased short term mortality. Our approach shows that metabolomic analysis of trial biorepositories according to response to intervention can yield important mechanistic insights and reveal patient populations who may or may not benefit.

Supplementary Material

Refer to Web version on PubMed Central for supplementary material.

Acknowledgements

This manuscript is dedicated to the memory of our dear friend and colleague Nathan Edward Hellman, MD, PhD.

Funding sources

The VITdAL-ICU trial was supported by the European Society for Clinical Nutrition and Metabolism (ESPEN), a research grant including provision of study medication from Fresenius Kabi (Germany), and the Austrian National Bank (Jubiläumsfonds, Project Nr. 14143). The metabolomics work was supported by the National Institutes of Health / National Institute of General Medical Sciences [R01 GM115774].

List of non-standard abbreviations

VITdAL-ICU trial	Correction of Vitamin D Deficiency in Critically Ill Patients trial
OPLS-DA	orthogonal partial least square-discriminant analysis
CV-ANOVA	cross-validation analysis of variance
FDR	False Discovery Rate
ITT	Intention-to-treat

References

- [1]. Kiehntopf M, Nin N, Bauer M. Metabolism, metabolome, and metabolomics in intensive care: is it time to move beyond monitoring of glucose and lactate? *Am J Respir Crit Care Med*. 2013;187:906–7. [PubMed: 23634857]
- [2]. Langley RJ, Tipper JL, Bruse S, Baron RM, Tsalik EL, Huntley J, et al. Integrative “omic” analysis of experimental bacteremia identifies a metabolic signature that distinguishes human sepsis from systemic inflammatory response syndromes. *Am J Respir Crit Care Med*. 2014;190:445–55. [PubMed: 25054455]
- [3]. Amrein K, Schnedl C, Holl A, Riedl R, Christopher KB, Pachler C, et al. Effect of high-dose vitamin D3 on hospital length of stay in critically ill patients with vitamin D deficiency: the VITdAL-ICU randomized clinical trial. *JAMA*. 2014;312:1520–30. [PubMed: 25268295]
- [4]. Lasky-Su J, Dahlin A, Litonjua AA, Rogers AJ, McGeachie MJ, Baron RM, et al. Metabolome alterations in severe critical illness and vitamin D status. *Crit Care*. 2017;21:193. [PubMed: 28750641]
- [5]. Tuoresmaki P, Vaisanen S, Neme A, Heikkinen S, Carlberg C. Patterns of genome-wide VDR locations. *PLoS One*. 2014;9:e96105. [PubMed: 24787735]
- [6]. Katajamaa M, Oresic M. Data processing for mass spectrometry-based metabolomics. *J Chromatogr A*. 2007;1158:318–28. [PubMed: 17466315]
- [7]. van den Berg RA, Hoefsloot HC, Westerhuis JA, Smilde AK, van der Werf MJ. Centering, scaling, and transformations: improving the biological information content of metabolomics data. *BMC Genomics*. 2006;7:142. [PubMed: 16762068]
- [8]. Sumner LW, Amberg A, Barrett D, Beale MH, Beger R, Daykin CA, et al. Proposed minimum reporting standards for chemical analysis Chemical Analysis Working Group (CAWG) Metabolomics Standards Initiative (MSI). *Metabolomics*. 2007;3:211–21. [PubMed: 24039616]
- [9]. Chong J, Soufan O, Li C, Caraus I, Li S, Bourque G, et al. MetaboAnalyst 4.0: towards more transparent and integrative metabolomics analysis. *Nucleic acids research*. 2018;46:W486–W94. [PubMed: 29762782]
- [10]. Westerhuis JA, Hoefsloot HCJ, Smit S, Vis DJ, Smilde AK, van Velzen EJJ, et al. Assessment of PLS-DA cross validation. *Metabolomics* 2008;4:81–9.
- [11]. Eriksson L, Trygg J, Wold S. CV-ANOVA for significance testing of PLS and OPLS models. *Journal of Chemometrics*. 2008;22:594–600.
- [12]. Krzywinski M, Schein J, Birol I, Connors J, Gascoyne R, Horsman D, et al. Circos: an information aesthetic for comparative genomics. *Genome Res*. 2009;19:1639–45. [PubMed: 19541911]
- [13]. Storey JD, Tibshirani R. Statistical significance for genomewide studies. *Proc Natl Acad Sci U S A*. 2003;100:9440–5. [PubMed: 12883005]
- [14]. Henglin M, Niiranen T, Watrous JD, Lagerborg KA, Antonelli J, Claggett BL, et al. A Single Visualization Technique for Displaying Multiple Metabolite-Phenotype Associations. *Metabolites*. 2019;9.
- [15]. Dustin T, Yamamoto T, Hirose K, Keele L, Imai K. mediation: R package for causal mediation analysis. *Journal of Statistical Software*. 2014;59:1–38. [PubMed: 26917999]
- [16]. Masuch A, Pietzner M, Bahls M, Budde K, Kastenmuller G, Zylla S, et al. Metabolomic profiling implicates adiponectin as mediator of a favorable lipoprotein profile associated with NT-proBNP. *Cardiovasc Diabetol*. 2018;17:120. [PubMed: 30153838]
- [17]. Pietzner M, Budde K, Homuth G, Kastenmuller G, Henning AK, Artati A, et al. Hepatic Steatosis Is Associated With Adverse Molecular Signatures in Subjects Without Diabetes. *J Clin Endocrinol Metab*. 2018;103:3856–68. [PubMed: 30060179]
- [18]. Laffey JG, Kavanagh BP. Negative trials in critical care: why most research is probably wrong. *Lancet Respir Med*. 2018;6:659–60. [PubMed: 30061048]
- [19]. Aberegg SK, Richards DR, O’Brien JM. Delta inflation: a bias in the design of randomized controlled trials in critical care medicine. *Crit Care*. 2010;14:R77. [PubMed: 20429873]
- [20]. Aberegg S Challenging orthodoxy in critical care trial design: physiological responsiveness. *Ann Transl Med*. 2016;4:147. [PubMed: 27162797]

- [21]. National Heart L, Blood Institute PCTN, Ginde AA, Brower RG, Caterino JM, Finck L, et al. Early High-Dose Vitamin D3 for Critically Ill, Vitamin D-Deficient Patients. *N Engl J Med*. 2019.
- [22]. Amrein K, Sourij H, Wagner G, Holl A, Pieber TR, Smolle KH, et al. Short-term effects of high-dose oral vitamin D3 in critically ill vitamin D deficient patients: a randomized, double-blind, placebo-controlled pilot study. *Crit Care*. 2011;15:R104. [PubMed: 21443793]
- [23]. Murnane PM, Brown ER, Donnell D, Coley RY, Mugo N, Mujugira A, et al. Estimating efficacy in a randomized trial with product nonadherence: application of multiple methods to a trial of preexposure prophylaxis for HIV prevention. *Am J Epidemiol*. 2015;182:848–56. [PubMed: 26487343]
- [24]. Preiser JC, Christopher K. High-Dose Vitamin D3 for Critically Ill Vitamin D-Deficient Patients. *N Engl J Med*. 2020;382:1670.
- [25]. Wallner S, Schmitz G. Plasmalogens the neglected regulatory and scavenging lipid species. *Chem Phys Lipids*. 2011;164:573–89. [PubMed: 21723266]
- [26]. Colombo S, Melo T, Martinez-Lopez M, Carrasco MJ, Domingues MR, Perez-Sala D, et al. Phospholipidome of endothelial cells shows a different adaptation response upon oxidative, glycative and lipoxidative stress. *Sci Rep*. 2018;8:12365. [PubMed: 30120318]
- [27]. Ahn WG, Jung JS, Song DK. Lipidomic analysis of plasma lipids composition changes in septic mice. *Korean J Physiol Pharmacol*. 2018;22:399–408. [PubMed: 29962854]
- [28]. Mueller RB, Sheriff A, Gaipl US, Wesselborg S, Lauber K. Attraction of phagocytes by apoptotic cells is mediated by lysophosphatidylcholine. *Autoimmunity*. 2007;40:342–4. [PubMed: 17516225]
- [29]. Schuster I Cytochromes P450 are essential players in the vitamin D signaling system. *Biochim Biophys Acta*. 2011;1814:186–99. [PubMed: 20619365]
- [30]. Gascon-Barre M, Demers C, Mirshahi A, Neron S, Zalzal S, Nanci A. The normal liver harbors the vitamin D nuclear receptor in nonparenchymal and biliary epithelial cells. *Hepatology*. 2003;37:1034–42. [PubMed: 12717384]
- [31]. Ding N, Yu RT, Subramaniam N, Sherman MH, Wilson C, Rao R, et al. A vitamin D receptor/SMAD genomic circuit gates hepatic fibrotic response. *Cell*. 2013;153:601–13. [PubMed: 23622244]
- [32]. Okazaki T, Bell RM, Hannun YA. Sphingomyelin turnover induced by vitamin D3 in HL-60 cells. Role in cell differentiation. *J Biol Chem*. 1989;264:19076–80. [PubMed: 2808413]
- [33]. Mueller M, Atanasov A, Cima I, Corazza N, Schoonjans K, Brunner T. Differential regulation of glucocorticoid synthesis in murine intestinal epithelial versus adrenocortical cell lines. *Endocrinology*. 2007;148:1445–53. [PubMed: 17170096]
- [34]. Lauber K, Bohn E, Krober SM, Xiao YJ, Blumenthal SG, Lindemann RK, et al. Apoptotic cells induce migration of phagocytes via caspase-3-mediated release of a lipid attraction signal. *Cell*. 2003;113:717–30. [PubMed: 12809603]
- [35]. Peter C, Waibel M, Radu CG, Yang LV, Witte ON, Schulze-Osthoff K, et al. Migration to apoptotic “find-me” signals is mediated via the phagocyte receptor G2A. *J Biol Chem*. 2008;283:5296–305. [PubMed: 18089568]
- [36]. Wang TJ, Larson MG, Vasan RS, Cheng S, Rhee EP, McCabe E, et al. Metabolite profiles and the risk of developing diabetes. *Nature medicine*. 2011;17:448–53.
- [37]. Koves TR, Ussher JR, Noland RC, Slentz D, Mosedale M, Ilkayeva O, et al. Mitochondrial overload and incomplete fatty acid oxidation contribute to skeletal muscle insulin resistance. *Cell Metab*. 2008;7:45–56. [PubMed: 18177724]
- [38]. Ryan ZC, Craig TA, Folmes CD, Wang X, Lanza IR, Schaible NS, et al. 1alpha,25-Dihydroxyvitamin D3 Regulates Mitochondrial Oxygen Consumption and Dynamics in Human Skeletal Muscle Cells. *J Biol Chem*. 2016;291:1514–28. [PubMed: 26601949]
- [39]. Ji L, Gupta M, Feldman BJ. Vitamin D Regulates Fatty Acid Composition in Subcutaneous Adipose Tissue Through Elov13. *Endocrinology*. 2016;157:91–7. [PubMed: 26488808]
- [40]. Sinha A, Hollingsworth KG, Ball S, Cheetham T. Improving the vitamin D status of vitamin D deficient adults is associated with improved mitochondrial oxidative function in skeletal muscle. *J Clin Endocrinol Metab*. 2013;98:E509–13. [PubMed: 23393184]

- [41]. Larson MC, Woodliff JE, Hillery CA, Kears TJ, Zhao M. Phosphatidylethanolamine is externalized at the surface of microparticles. *Biochim Biophys Acta*. 2012;1821:1501–7. [PubMed: 22960380]
- [42]. de Boland AR, Boland R. Suppression of 1,25-dihydroxy-vitamin D3-dependent calcium transport by protein synthesis inhibitors and changes in phospholipids in skeletal muscle. *Biochim Biophys Acta*. 1985;845:237–41. [PubMed: 2581623]
- [43]. Milgrom H, Curran-Everett D. Unrecognized nonadherence masquerades as drug resistance. *Curr Opin Allergy Clin Immunol*. 2012;12:219–20. [PubMed: 22517289]
- [44]. Oberg AL, Mahoney DW. Linear mixed effects models. *Methods Mol Biol*. 2007;404:213–34. [PubMed: 18450052]
- [45]. Ernest B, Gooding JR, Campagna SR, Saxton AM, Voy BH. MetabR: an R script for linear model analysis of quantitative metabolomic data. *BMC Res Notes*. 2012;5:596. [PubMed: 23111096]
- [46]. Xia J, Sinelnikov IV, Wishart DS. MetATT: a web-based metabolomics tool for analyzing time-series and two-factor datasets. *Bioinformatics*. 2011;27:2455–6. [PubMed: 21712247]
- [47]. Little RJ, Long Q, Lin X. A comparison of methods for estimating the causal effect of a treatment in randomized clinical trials subject to noncompliance. *Biometrics*. 2009;65:640–9. [PubMed: 18510650]

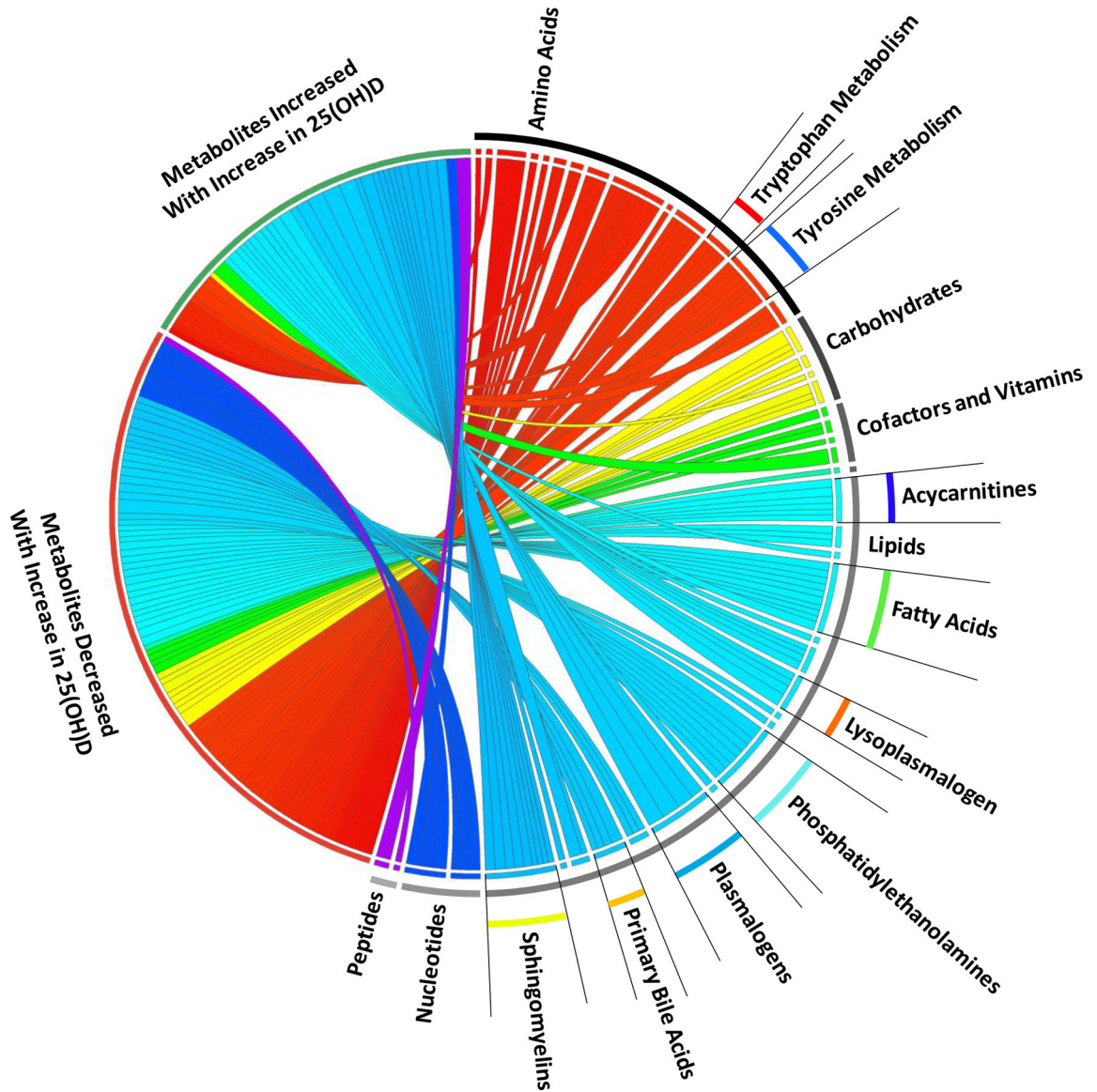


Figure 1. Circos plot of plasma metabolites by absolute increase in 25(OH)D levels. Bipartite graph illustrating mixed-effects linear regression results of metabolites with significantly changes (increased or decreased) over day 0, 3 and 7 with an absolute increase in 25(OH)D levels between day 0 and day 3. Graph connects metabolic response to an absolute increase in 25(OH)D levels with the individual metabolites grouped by metabolite Super Pathway (e.g. lipid) and Sub Pathway (e.g. sphingomyelin). Width of curves indicates strength of the significance ($-\log_{10}(p)$ value) with wider curves having greater significance. All metabolites shown are significant at the $-\log_{10}(p) > 4.06$, $p < 8.65 \times 10^{-5}$ level.

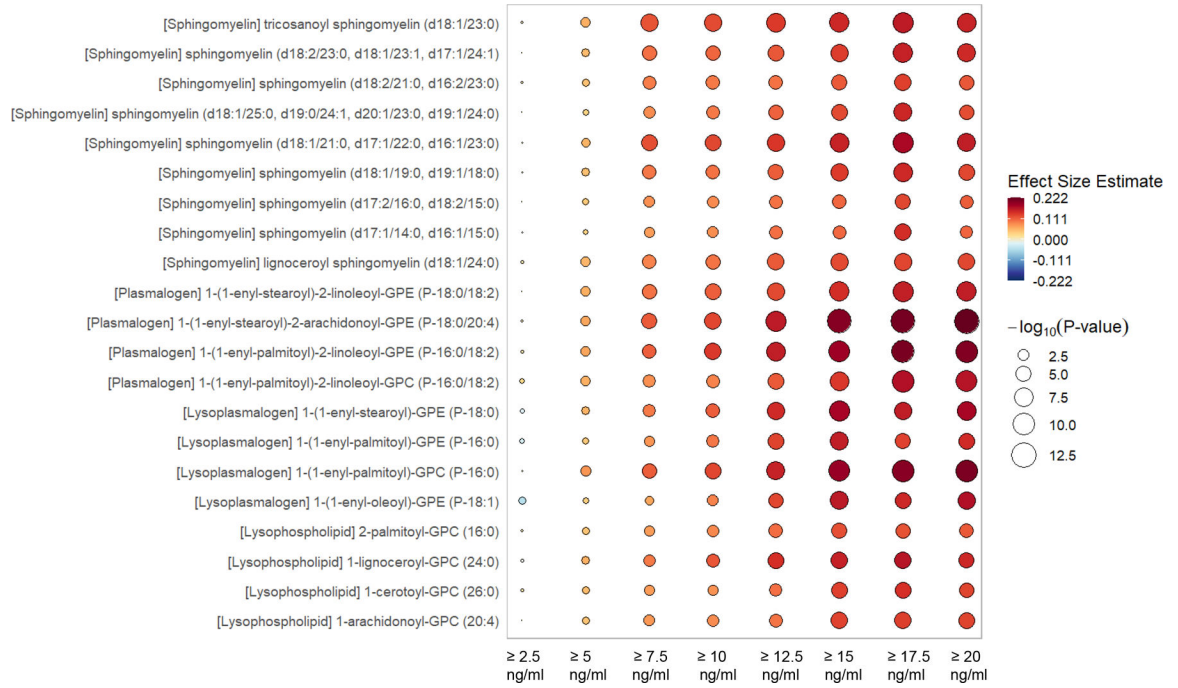


Figure 2. Rain plot of increasing metabolites by incremental absolute increase in 25(OH)D following intervention. The rain plot shows the directionality and magnitude of estimates of the association between individual metabolites and the absolute increase of plasma 25(OH)D between day 0 and day 3 to levels of $\geq 2.5, 5.0, 7.5, 10.0, 12.5, 15.0, 17.5$ or 20.0 ng/ml. Results are focused on sphingomyelins, plasmalogens, lysoplasmalogen and lysophospholipids. The color fill scale of individual rain plots indicates the effect size - increased (dark red) or decreased (dark blue) of the individual metabolite following mixed-effects linear regression. The size of the individual rain ‘droplet’ indicates strength of the significance ($-\log_{10}(p)$) with larger plots having greater significance. Metabolites shown are considered significant at the $-\log_{10}(p) > 4.06, p < 8.65 \times 10^{-5}$ level.

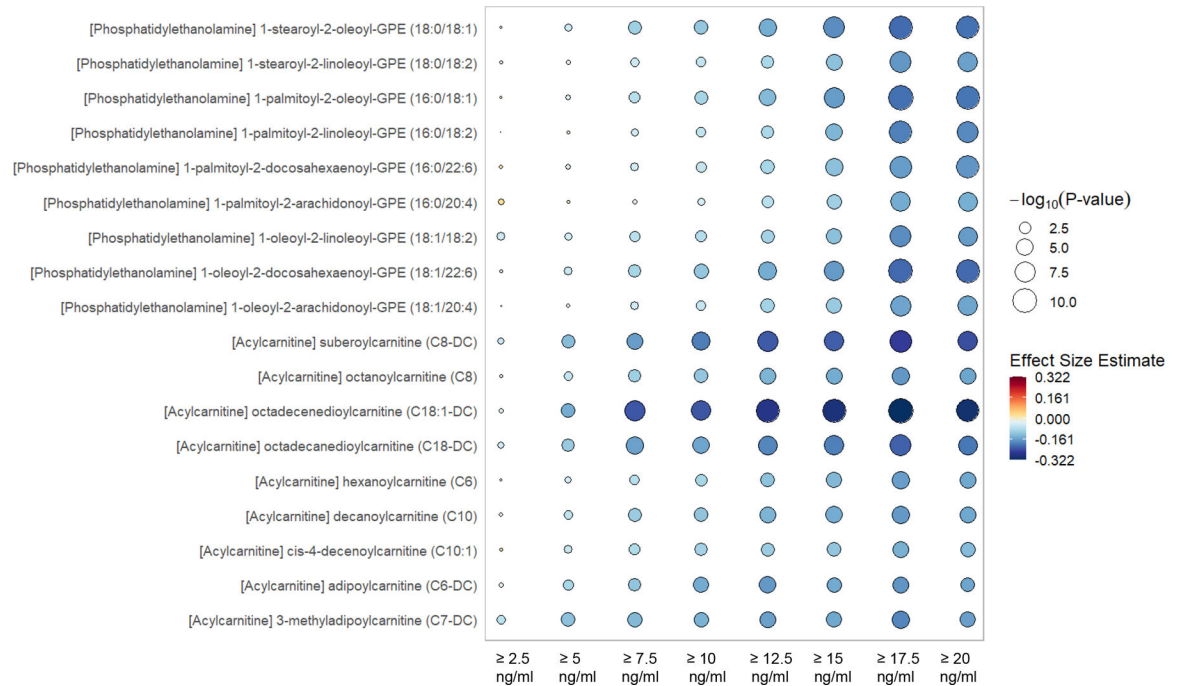


Figure 3.

Rain plot of decreasing metabolites by incremental absolute increase in 25(OH)D following intervention. The rain plot shows the directionality and magnitude of estimates of the association between individual metabolites and the absolute increase of plasma 25(OH)D between day 0 and day 3 to levels of ≥ 2.5 , ≥ 5.0 , ≥ 7.5 , ≥ 10.0 , ≥ 12.5 , ≥ 15.0 , ≥ 17.5 or ≥ 20.0 ng/ml. Results are focused on acylcarnitines and phosphatidylethanolamines. The color fill scale of individual rain plots indicates the effect size - increased (dark red) or decreased (dark blue) of the individual metabolite following mixed-effects linear regression. The size of the individual rain ‘droplet’ indicates strength of the significance ($-\log_{10}(p)$ value) with larger plots having greater significance. Metabolites shown are considered significant at the $-\log_{10}(p) > 4.06$, $p < 8.65 \times 10^{-5}$ level.

Table 1.

Cohort Characteristics

Characteristic	Absolute increase in 25(OH)D between day 0 and day 3				Total	P-value
	<0.0 ng/ml	0.0–3.14 ng/ml	3.15–16.40 ng/ml	> 16.40 ng/ml		
No. (%)	105	109	107	107	428	
Age Mean (SD)	62.7 (14.7)	65.9 (12.7)	64.6 (14.6)	63.4 (17.3)	64.2 (14.9)	0.42*
Female Sex No. (%)	38 (36.2)	36 (33.0)	36 (33.6)	41 (38.3)	151 (35.3)	0.84
Day 0 25(OH)D Mean (SD)	14.6 (4.6)	12.5 (4.8)	12.3 (4.2)	13.3 (4.7)	13.2 (4.6)	0.001*
SAPS II Mean (SD)	31.3 (13.4)	35.1 (14.7)	33.6 (15.9)	33.4 (17.2)	33.4 (15.4)	0.34*
CRP Day 0 Mean (SD)	116.5 (86.1)	128.7 (83.7)	137.8 (90.2)	116.2 (98.0)	124.9 (89.8)	0.23*
Total Bilirubin Day 0 Mean (SD)	1.8 (4.1)	1.5 (1.8)	2.0 (2.4)	1.0 (1.5)	1.6 (2.6)	0.026*
Creatinine Day 0 Mean (SD)	1.5 (1.2)	1.4 (1.0)	1.5 (1.0)	1.2 (0.8)	1.4 (1.0)	0.036*
Vitamin D ₃ Intervention No. (%)	18 (17.1)	17 (15.6)	70 (65.4)	107 (100)	212 (49.5)	<0.001
ICU						<0.001
Anesthesia ICU No. (%)	28 (26.7)	22 (20.2)	16 (15.0)	17 (15.9)	83 (19.4)	
Cardiac Surgery ICU No. (%)	27 (25.7)	40 (36.7)	39 (36.5)	20 (18.7)	126 (29.4)	
Surgical ICU No. (%)	5 (4.8)	3 (2.8)	10 (9.4)	5 (4.7)	23 (5.4)	
Medicine ICU No. (%)	27 (25.7)	20 (18.4)	22 (20.6)	21 (19.6)	90 (21.0)	
Neurological ICU No. (%)	18 (17.1)	24 (22.0)	20 (18.7)	44 (41.1)	106 (24.8)	
28-day Mortality No. (%)						
Analytic Cohort (N=428)	28 (26.7)	29 (26.6)	29 (27.1)	9 (8.4)	95 (22.2)	0.001
Baseline 25(OH)D ≥ 12 ng/ml (N=181)	13 (40.6)	18 (36.0)	12 (23.5)	4 (8.3)	47 (26.0)	0.003

Note: Data presented as n (%) unless otherwise indicated. P values determined by chi-square unless designated by (*) then P value determined by ANOVA

Table 2.

Highlighted Metabolites significantly increased with an Increase in 25(OH)D

Metabolite	P-value	Bonferroni corrected P-value	-log10p	β Coefficient	Super Pathway	Sub Pathway
1-lignoceroyl-GPC (24:0)	3.27 E-07	1.89 E-04	6.49	0.0047	Lipid	Lysophospholipid
1-cerotoyl-GPC (26:0) *	2.11 E-06	1.22 E-03	5.67	0.0038	Lipid	Lysophospholipid
2-palmitoyl-GPC (16:0) *	5.49 E-05	3.17 E-02	4.26	0.0031	Lipid	Lysophospholipid
1-arachidonoyl-GPC (20:4) *	5.37 E-05	3.10 E-02	4.27	0.0030	Lipid	Lysophospholipid
1-(1-enyl-palmitoyl)-GPC (P-16:0) *	1.08 E-10	6.26 E-08	9.97	0.0054	Lipid	Lysoplasmalogen
1-(1-enyl-stearoyl)-GPE (P-18:0) *	1.57 E-08	9.06 E-06	7.80	0.0047	Lipid	Lysoplasmalogen
1-(1-enyl-oleoyl)-GPE (P-18:1) *	4.32 E-06	2.50 E-03	5.36	0.0041	Lipid	Lysoplasmalogen
1-(1-enyl-palmitoyl)-GPE (P-16:0) *	2.86 E-06	1.65 E-03	5.54	0.0039	Lipid	Lysoplasmalogen
1-(1-enyl-palmitoyl)-2-linoleoyl-GPE (P-16:0/18:2) *	4.02 E-14	2.32 E-11	13.40	0.0063	Lipid	Plasmalogen
1-(1-enyl-stearoyl)-2-arachidonoyl-GPE (P-18:0/20:4) *	5.79 E-15	3.35 E-12	14.24	0.0061	Lipid	Plasmalogen
1-(1-enyl-stearoyl)-2-linoleoyl-GPE (P-18:0/18:2) *	8.42 E-14	4.87 E-11	13.07	0.0053	Lipid	Plasmalogen
1-(1-enyl-palmitoyl)-2-linoleoyl-GPC (P-16:0/18:2) *	8.62 E-11	4.98 E-08	10.06	0.0046	Lipid	Plasmalogen
Sphingomyelin (d18:1/21:0, d17:1/22:0, d16:1/23:0) *	2.01 E-08	1.16 E-05	7.70	0.0044	Lipid	Sphingomyelins
Tricosanoyl sphingomyelin (d18:1/23:0) *	2.79 E-09	1.61 E-06	8.55	0.0043	Lipid	Sphingomyelins
Sphingomyelin (d18:2/23:0, d18:1/23:1, d17:1/24:1) *	7.85 E-08	4.54 E-05	7.11	0.0039	Lipid	Sphingomyelins
Lignoceroyl sphingomyelin (d18:1/24:0)	2.15 E-08	1.24 E-05	7.67	0.0038	Lipid	Sphingomyelins
Sphingomyelin (d18:1/19:0, d19:1/18:0) *	4.61 E-07	2.66 E-04	6.34	0.0037	Lipid	Sphingomyelins
Sphingomyelin (d17:1/14:0, d16:1/15:0) *	3.14 E-05	1.82 E-02	4.50	0.0034	Lipid	Sphingomyelins
Sphingomyelin (d18:1/25:0, d19:0/24:1, d20:1/23:0, d19:1/24:0) *	4.65 E-05	2.69 E-02	4.33	0.0031	Lipid	Sphingomyelins
Sphingomyelin (d17:2/16:0, d18:2/15:0) *	5.97 E-05	3.45 E-02	4.22	0.0031	Lipid	Sphingomyelins
Sphingomyelin (d18:2/21:0, d16:2/23:0) *	4.15 E-05	2.40 E-02	4.38	0.0030	Lipid	Sphingomyelins

Note: Increase in 25(OH)D is defined as the absolute ng/ml increase in plasma 25(OH)D from baseline day 0 to day 3 following randomization.

* indicates the metabolite has a recognized identification with predictive or externally acquired structure evidence. All other Metabolites have validated identification against a pure reference standard. GPC is glycerylphosphorylcholine; GPE is glycerophosphoethanolamine. All significant mixed-effects associations have P-value < 8.65×10^{-5} .

Table 3.

Highlighted Metabolites significantly decreased with an Increase in 25(OH)D

Metabolite	P-value	Bonferroni corrected P-value	-log ₁₀ p	β Coef.	Super Pathway	Sub Pathway
Malonylcarnitine (C3-DC)	6.84 E-06	3.95 E-03	5.16	-0.0038	Lipid	Acylcarnitines
2-methylmalonylcarnitine (C4-DC)	3.40 E-06	1.97 E-03	5.47	-0.0050	Lipid	Acylcarnitines
Succinylcarnitine (C4-DC)	7.05 E-05	4.07 E-02	4.15	-0.0034	Lipid	Acylcarnitines
3-methyladipoylcarnitine (C7-DC)	1.05 E-05	6.04 E-03	4.98	-0.0047	Lipid	Acylcarnitines
Suberoylcarnitine (C8-DC)	8.64 E-08	5.00 E-05	7.06	-0.0063	Lipid	Acylcarnitines
Octadecenedioylcarnitine (C18:1-DC)*	2.07 E-07	1.20 E-04	6.68	-0.0067	Lipid	Acylcarnitines
Octadecanedioylcarnitine (C18-DC)*	4.72 E-05	2.73 E-02	4.33	-0.0042	Lipid	Acylcarnitines
1-oleoyl-2-linoleoyl-GPE (18:1/18:2)*	3.35 E-07	1.94 E-04	6.47	-0.0042	Lipid	Phosphatidylethanolamine
1-stearoyl-2-oleoyl-GPE (18:0/18:1)	9.63 E-07	5.57 E-04	6.02	-0.0043	Lipid	Phosphatidylethanolamine
1-oleoyl-2-docosahexaenoyl-GPE (18:1/22:6)*	1.00 E-11	5.78 E-09	11.00	-0.0059	Lipid	Phosphatidylethanolamine
1-stearoyl-2-linoleoyl-GPE (18:0/18:2)*	1.15 E-05	6.65 E-03	4.94	-0.0034	Lipid	Phosphatidylethanolamine
1-oleoyl-2-arachidonoyl-GPE (18:1/20:4)*	1.14 E-06	6.58 E-04	5.94	-0.0036	Lipid	Phosphatidylethanolamine
1-palmitoyl-2-linoleoyl-GPE (16:0/18:2)	4.32 E-06	2.50 E-03	5.36	-0.0038	Lipid	Phosphatidylethanolamine
1-palmitoyl-2-docosahexaenoyl-GPE (16:0/22:6)*	1.52 E-07	8.76 E-05	6.82	-0.0038	Lipid	Phosphatidylethanolamine
1-palmitoyl-2-oleoyl-GPE (16:0/18:1)	1.76 E-07	1.02 E-04	6.75	-0.0043	Lipid	Phosphatidylethanolamine
Indolelactate	5.77 E-05	3.34 E-02	4.24	-0.0035	Amino Acid	Tryptophan Metabolism
Kynurenate	1.32 E-05	7.62 E-03	4.88	-0.0057	Amino Acid	Tryptophan Metabolism
N-acetyltryptophan	1.90 E-08	1.10 E-05	7.72	-0.0177	Amino Acid	Tryptophan Metabolism
3-(4-hydroxyphenyl)lactate	4.54 E-05	2.62 E-02	4.34	-0.0037	Amino Acid	Tyrosine Metabolism
N-acetyltyrosine	3.85 E-05	2.22 E-02	4.41	-0.0047	Amino Acid	Tyrosine Metabolism
3-methoxytyramine sulfate	1.52 E-05	8.79 E-03	4.82	-0.0049	Amino Acid	Tyrosine Metabolism
Homovanillate	1.23 E-06	7.09 E-04	5.91	-0.0050	Amino Acid	Tyrosine Metabolism
Vanillylmandelate	1.12 E-06	6.46 E-04	5.95	-0.0056	Amino Acid	Tyrosine Metabolism
Homovanillate sulfate	1.45 E-06	8.40 E-04	5.84	-0.0066	Amino Acid	Tyrosine Metabolism

Note: Increase in 25(OH)D is defined as the absolute ng/ml increase in plasma 25(OH)D from baseline day 0 to day 3 following randomization.

* indicates the metabolite has a recognized identification with predictive or externally acquired structure evidence. All other Metabolites have validated identification against a pure reference standard. GPC is glycerylphosphorylcholine; GPE is glycerophosphoethanolamine. For the Acylcarnitine sub pathway: a capital C is followed by the number of carbons within the fatty acyl group attached to the carnitine. A colon followed by a number is one or more unsaturated carbons in the acylcarnitine ester (i.e. C10:1 is a monounsaturated C10 acylcarnitine). DC following the carbon number is a dicarboxylic acylcarnitine. All significant mixed-effects associations have P-value < 8.65×10^{-5} .